Inorg. Chem. **2004**, *43*, 3142–3150

Assignment of the Electronic Spectra of $[Mo(CN)_8]^{4-}$ and $[W(CN)_8]^{4-}$ by Ab Initio Calculations

M. F. A. Hendrickx,*,† V. S. Mironov,‡ L. F. Chibotaru,† and A. Ceulemans†

Department of Chemistry, University of Leuven, Celestijnenlaan 200F, B-3001 Leuven, Belgium, and Institute of Crystallography, Russian Academy of Sciences, Leninskii Prosp. 59, 117333 Moscow, Russia

Received November 6, 2003

CASPT2 calculations are performed on the dodecahedral and square antiprismatic isomers of the $[Mo(CN)_8]^{4-}$ and $[W(CN)_8]^{4-}$ complexes. The high-energy experimental bands above 40000 cm^{-1} are assigned to MLCT transitions. The experimental observed trend of the extinction coefficients for the molybdenum and tungsten complex is reproduced by our CASSCF oscillator strengths. All bands below 40000 cm^{-1} can be ascribed to ligand-field transitions, although small contributions from forbidden MLCT transitions cannot be excluded. In order to account for all experimental bands in the electronic spectrum of these octacyanocomplexes, a dynamic equilibrium in solution between the two isomeric forms must be hypothesized. Spin–orbit coupling effects are found to be more important for the square antiprismatic isomers; in particular, large singlet–triplet mixings are calculated for this isomer of $[W(CN)_8]^{4-}$. Ligand-field and Racah parameters as well as spin–orbit coupling constants are determined on the basis of the calculated transition energies. The obtained values for these parameters support the recently proposed model for exchange interactions in magnetic clusters and networks containing pentavalent octocyanometalates of molybdenum and tungsten.

Introduction

During the past years interest in the cyanocomplexes was revived due to the fact that they are building blocks of magnetic clusters and networks.[1−11] They are of potential importance for the development of single molecule magnets. It has been shown that the incorporation in cyano-bridged compounds of second- and third-row transition metal cations with diffuse d valence orbitals leads[12−14] to strong magnetic exchange couplings between the metal centers. A thorough understanding of the origin of the ferromagnetic coupling is currently the subject of theoretical research. Beside quantum chemical investigations,[15−17] models for kinetic exchange interaction based on Anderson's theory of superexchange[18] have also been proposed.[19−21] The efficiency of the model

* To whom correspondence should be addressed. E-mail: marc.hendrickx@chem.kuleuven.ac.be.
† University of Leuven.
‡ Russian Academy of Sciences.

(1) Mallah, T.; Auberger, C.; Verdaguer, M.; Veillet, P. *J. Chem. Soc., Chem. Commun.* **1995**, 61.
(2) El Fallah, S. M.; Rentschler, E.; Caneschi, A.; Sessoli, R.; Gatteschi, D. *Angew. Chem.* **1996**, *108*, 2081−2083; *Angew. Chem., Int. Ed. Engl.* **1996**, *35*, 1947.
(3) Scuiller, A.; Mallah, T.; Verdaguer, M.; Nivorozhkin, A.; Tholence, J.-L.; Veillet, P. *New J. Chem.* **1996**, *20*, 1.
(4) Heinrich, J. L.; Berseth, P A.; Long, J. R. *J. Chem. Soc., Chem. Commun.* **1998**, 1231.
(5) Ferlay, S.; Mallah, T.; Quahès, R.; Velliet, P.; Verdaguer, M. *Inorg. Chem.* **1999**, *38*, 229.
(6) Mallah, T.; Marvilliers, A.; Rivière, E. *Phil. Trans. R. Soc. London, Ser. A* **1999**, *357*, 3139.
(7) Griebler, W.-D.; Babel, D. *Z. Naturforsch., B: Chem. Sci.* **1982**, *37*, 832.
(8) Gadet, V.; Mallah, T.; Castro, I.; Verdaguer, M.; Veillet, P. *J. Am. Chem. Soc.* **1992**, *114*, 9213.
(9) Mallah, T.; Thiebaut, S.; Verdaguer, M.; Veillet, P. *Science* **1993**, *262*, 1554−1557.
(10) Ferlay, S.; Mallah, T.; Quahès, R.; Veillet, P.; Verdaguer, M. *Nature* **1995**, *378*, 701.
(11) Holmes, S. M.; Girolami, G. S. *J. Am. Chem. Soc.* **1999**, *121*, 5593.
(12) Shores, M. P.; Sokol, J. J.; Long, J. R. *J. Am. Chem. Soc.* **2002**, *124*, 2279.
(13) Sokol, J. J.; Hee, A. G.; Long, J. R. *J. Am. Chem. Soc.* **2002**, *124*, 7656.
(14) Bennett, M. V.; Long, J. R. *J. Am. Chem. Soc.* **2003**, *125*, 2394.
(15) Eyert, V.; Siberchicat, B.; Verdaguer, M. *Phys. Rev. B* **1997**, *56*, 8959.
(16) Harrison, N. M.; Searle, B. G.; Seddon, E. A. *Chem. Phys. Lett.* **1997**, *266*, 507.
(17) Nishino, M.; Yoshioko, Y.; Yamaguchi, K. *Chem. Phys. Lett.* **1998**, *297*, 51.
(18) Anderson, P. W. *Phys. Rev. B* **1959**, *115*, 2.
(19) Weihe, H.; Güdel, H. U. *Comments Inorg. Chem.* **2000**, *22*, 75.
(20) Chibotaru, L. F.; Mironov, V. S.; Ceulemans, A. *Angew. Chem., Int. Ed.* **2001**, *40*, 4429.
(21) Mironov, V. S.; Chibotaru, L. F.; Ceulemans, A. *J. Am. Chem. Soc.* **2003**, *125*, 9750.

10.1021/ic035282t CCC: $27.50
Published on Web 04/14/2004

therefore depends strongly on the quality of the parameters. The values for these parameters were often derived several decades ago on the basis of wrong assignations of the experimental spectra of the corresponding mononuclear complexes, as has recently been proven by us for the d^1 complex $[Mo(CN)_8]^{3-}$.[22,23] In the present contribution, we extend our ab intio study to the spectra of the related d^2 complexes $[Mo(CN)_8]^{4-}$ and $[W(CN)_8]^{4-}$, which will allow us to derive Racah repulsion parameters.

$[Mo(CN)_8]^{4-}$ and $[W(CN)_8]^{4-}$ cyanometalates serve frequently as textbook examples of octacoordinated complexes.[24,25] In crystals, these complexes possess either dodecahedral or square antiprismatic structures,[26−38] the actual structure depending on the specific counterions involved. In solution, the situation is less clear. For the two title complexes, the experimental UV−vis spectra in aqueous solutions were first reported by Perumareddi et al.[22] In the same paper, an assignment of the spectra is given on the basis of the assumption of a dodecahedral structure for both complex anions. Later, an NMR study[39] of aqueous solutions of $K_4[Mo(CN)_8]$ and magnetic circular dichroism spectroscopy[40] on several $[W(CN)_8]^{4-}$ salts further indicated that the structure for both complex anions is dodecahedral. The assignment of Perumareddi et al. was later contested by Golebiewski et al.,[41] who proposed a square antiprismatic coordination geometry for $[Mo(CN)_8]^{4-}$. Both semiempirical treatments of the electronic structure agree in the sense that the low-energy bands of the spectra (<40000 cm^{-1}) find their origin in ligand-field transitions between the split d orbitals of the metal cations. In addition, these studies ascribe the high-energy bands to charge transfer transitions, which are further characterized by Golebiewski et al.[41] as an excitation of an electron from the lowest lying doubly occupied d orbital to an unoccupied ligand orbital (MLCT). Both Perumareddi et al.[22] and Golebiewski et al.,[41] made for the pentavalent d^1 complex $[Mo(CN)_8]^{3-}$ a similar assignment, i.e., ligand-field bands in the low-energy part and CT bands in high-energy part of the spectra (although of the inverse LMCT nature). Recently, a more rigorous ab initio treatment of the spectrum of the latter $[Mo(CN)_8]^{3-}$ complex clearly showed that at least for the d^1 complexes this picture of the electronic structure is incorrect.[23] State-of-the-art CASPT2 calculations on this complex arrived at a completely different assignment. All experimentally observed bands were ascribed to low-lying charge transfer states of the type LMCT of the dodecahedral isomer. Therefore, in view of these CASPT2 results for $[Mo(CN)_8]^{3-}$ a reassessment of the assignment of the spectra of the tetravalent $[Mo(CN)_8]^{4-}$ and $[W(CN)_8]^{4-}$ is necessary.

Table 1. Irreducible Representations of the d Orbitals for D_{4d}, D_{2d}, and the D_2 Point Groups

	D_{2d}	D_2		D_2	D_{4d}
z^2	a_1	a	z^2	a	a_1
x^2-y^2	b_1	a	x^2-y^2, xy	a, b_1	e_2
xy	b_2	b_1	xz, yz	b_2, b_3	e_3
xz, yz	e	b_2, b_3			

Computational Details

The D_{2d} and D_{4d} symmetry point groups of the respective dodecahedral and square antiprismatic geometries of the octacyanocomplexes have irreducible representations (irreps) that are degenerate and therefore are not directly usable in the MOLCAS suite of computer programs,[42] which can handle only point groups with nondegenerate irreps. For both isomers, the wave functions were calculated by imposing D_2 symmetry, inducing deviations in energies that are known to be small (a few 100 cm^{-1} maximum). Table 1 shows the correspondence between the D_{4d}, D_{2d}, and D_2 point groups for the irreps of the d orbitals of the metal cations. On the basis of crystallographic data, all bond distances Mo−C and C−N in our ab initio calculations are set equal to values of 2.16 and 1.15 Å,[26] respectively, while for the tungsten complexes, average W−C and C−N bond distances of 2.18 and 1.13 Å were chosen.[29] The M−C and C−N bonds are collinear for each ligand. For the dodecahedral isomers of the molybdenum and tungsten complexes, the two sets of cyanide ligands are placed at polar angle values of 37° and 70° (idealized dodecahedron corresponding to the closest ligand packing) with the principal S_4 axis (*z*-axis in Figure 1a); these two sets will be denoted as axial and equatorial ligands, respectively. In the square antiprism isomers, all cyanide ligands are symmetry equivalent, the polar angle with the S_8 principal axis (*z*-axis in Figure 1b) was put equal to 58°.[29]

In the previous studies of the spectra of transition metal complexes in general,[43−46] the CASPT2 method proved to be

(22) Perumareddi, J. R.; Liehr, A. D.; Adamson, A. W. *J. Am. Chem. Soc.* **1963**, *85*, 249.
(23) Hendrickx, M. F. A.; Chibotaru, L. F.; Ceulemans, A. *Inorg. Chem.* **2003**, *42*, 590.
(24) Cotton, F. A.; Wilkinson, G. *Advanced Inorganic Chemistry*, 5th ed.; John Wiley & Sons: New York, 1988.
(25) Prucell, K. F.; Kotz, J. C. *Inorganic Chemistry*; W. B. Saunders Company: Philadelphia, 1977.
(26) Hoard, J. L.; Hamor, T. A.; Glick, M. D. *J. Am. Chem. Soc.* **1968**, *90*, 3177.
(27) Corden, B. J.; Cunningham, J. A.; Eisenberg, R. *Inorg. Chem.* **1970**, *9*, 356.
(28) Bok, L. D. C.; Leipoldt, J. G.; Basson, S. S. *Acta Crystallogr.* **1970**, *B26*, 684.
(29) Basson, S. S.; Bok, L. D. C.; Leipoldt, J. G. *Acta Crystallogr.* **1970**, *B26*, 1209.
(30) Meske, W.; Babel, D. *Z. Anorg. Allg. Chem.* **1988**, *624*, 1751.
(31) Zhong, Z. J.; Seino, H.; Mizobe, Y.; Hidai, M.; Verdaguer, M.; Ohkoshi, S.; Hashimoto, K. *Inorg. Chem.* **2000**, *39*, 5095.
(32) Nadele, D.; Schweda, E. *Z. Kristallogr.* **1999**, *214*, 358.
(33) Sieklucka, B.; Lasocha, W.; Proniewicz, L. M.; Podgajny, R.; Schenk, H. *J. Mol. Struct.* **2000**, *520*, 155.
(34) Nowicka, B.; Samotus, A.; Szklarzewicz, J.; Burgess, J.; Fawcett, J.; Russell, D. R. *Polyhedron* **1998**, *17*, 3167.
(35) Meske, W.; Babel, D. *J. Alloys Compd.* **1992**, *183*, 158.
(36) Meske, W.; Babel, D. *Z. Naturforsch., B: Chem. Sci.* **1999**, *54*, 117.
(37) Meske, W.; Babel, D. *Z. Anorg. Allg. Chem.* **1999**, *625*, 51.
(38) Alcock, N. W.; Samotus, A.; Szklarzewicz, J. *J. Chem. Soc., Dalton Trans.* **1993**, *6*, 885.
(39) Brownlee, R. T. C.; Shehan, B. P.; Wedd, A. G. *Inorg. Chem.* **1987**, *26*, 2022.
(40) Pribush, R. A.; Archer, R. D. *Inorg. Chem.* **1974**, *13*, 2556.
(41) Golebiewski, A.; Kowalski, H. *Theor. Chim. Acta* **1968**, *12*, 293.
(42) Andersson, K.; Barysz, M.; Bernhardsson, A.; Blomberg, M. R.A.; Cooper, D. L.; Fülscher, M. P.; de Graaf, C.; Hess, B. A.; Karlström, G.; Lindh, R.; Malmqvist, P.-Å.; Nakajima, T.; Neogrády, P.; Olsen, J.; Roos, B. O.; Schimmelpfennig, B.; Schütz, M.; Seijo, L.; Serrano-Andrés, L.; Siegbahn, P. E. M.; Stålring, J.; Thorsteinsson, T.; Veryazov, V.; Widmark, P.-O. *Molcas* 5.4; Lund University: Sweden, 2002.
(43) Pierloot, K; Van Praet, E.; Vanquickenborne, L. G. *J. Phys. Chem.* **1993**, *90*, 87.
(44) Pierloot, K.; Tsokos, E.; Vanquickenborne, L. G. *J. Phys. Chem.* **1996**, *100*, 16545.
(45) Pierloot, K.; Ceulemans, A.; Merchan, M.; Serrano-Andrés, L. *J. Phys. Chem. A* **2000**, *104*, 4374.
(46) Ribbing, C.; Gilliams, B.; Pierloot, K.; Roos, B. O.; Karlstrom, G. *J. Chem. Phys.* **1998**, *109*, 3145.

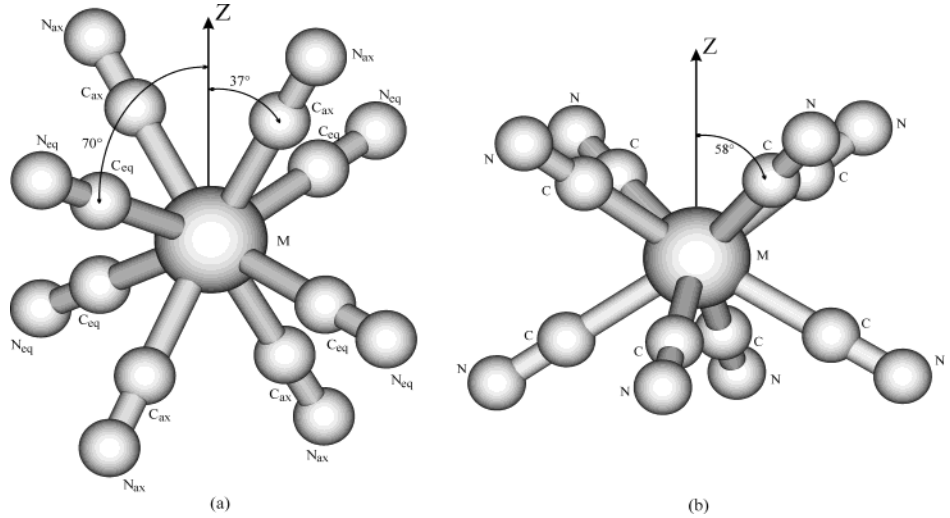

Figure 1. Dodecahedral (a) and square antiprismatic (b) structures as used in the calculations. For both isomers the *z* axis corresponds to the principal symmetry axis. *x* and *y* axes are defined in Figure 4.

reliable. In particular, the well-known and characterized ligand-field spectrum of $MoCl_6^{3-}$ has been accurately reproduced, whereas for the $Mo(CN)_6^{3-}$ a reasonable value for the 10*Dq* parameter is predicted.[47] Both for ligand-field and charge transfer transitions, the deviations of the transition energies between theory and experiment are generally smaller than 2000 cm^{-1}. In the present study, the ligand part is described by exactly the same atomic natural basis (ANO) set as the one used in our previous calculations on molybdenum cyanide complexes.[23] This also applies for the effective core potential (ECP) basis set used for the expansion of the orbitals occupied by the valence electrons of Mo^{4+}. For the valence orbitals (5p, 5d, and 6s) of W^{4+} a similar Barandiaran ECP basis set was selected,[48] which consists of three s, three p, four d, and two f contracted functions (as implemented in MOLCAS 5.4). Relativistic effects are accounted for by simulating the metal cores by the appropriate relativistic effective core potentials. Ligand-field states are calculated at the CASSCF level as individual roots, whereas because of the high density of charge transfer (CT) terms a state averaged CASSCF is performed for this type of states. The CASSCF treatment, which takes into account the most important near-degeneracy effects, yields orbitals that are subsequently used in a second-order perturbation (CASPT2) treatment of the dynamic electron correlation. Only the 1s electrons of C and N, and obviously the core electrons of molybdenum and tungsten (ECP basis), are excluded from the wave function expansion in the perturbation treatment. A total number of 88 electrons is correlated for the two isomeric structures of $[Mo(CN)_8]^{4-}$ and $[W(CN)_8]^{4-}$.

Of critical importance in a CASPT2 description of a wave function is the extent of the active space used in the CASSCF part of the calculation. An adequate choice requires some knowledge of the electronic structure of the system to be studied, in particular if the active space needs to be large. If such knowledge is not available, preliminary test calculations using different active spaces are needed in order to assess the most important contributions to the electronic wave functions. In the case of $[Mo(CN)_8]^{4-}$ and $[W(CN)_8]^{4-}$, it appeared that the 4d and 5d orbitals, respectively, are energetically placed between and almost at an equal distance from the occupied 1π and the unoccupied $2\pi^*$ orbitals of the cyanide ligand. Therefore, the ideal active space should include in addition to the metal d orbitals all 32 1π and $2\pi^*$ orbitals of the cyanide ligands, obviously an active space that is far too large to be handled by present-day computers and computational chemistry software. In order to circumvent this limitation, a reduction of the active space is needed. A procedure identical to the one applied in our CASPT2 study of the $[Mo(CN)_8]^{3-}$ complex,[23] and which was originally used with success for assigning the charge transfer spectrum of $Cr(CO)_6$,[44] will also be utilized for the description of the electronic structure of $[Mo(CN)_8]^{4-}$ and $[W(CN)_8]^{4-}$. Four different active spaces, one for each irrep of D_2, are constructed according to the following procedure. In addition to the five 4d (Mo) or 5d (W) orbitals, each of the four different active spaces includes 4 linear combinations of the occupied 1π and 4 linear combinations of the unoccupied $2\pi^*$ ligand orbitals that transform according to that specific irrep. Regardless of spin multiplicity, the wave function of each electronic state for which the spatial part transforms according to a particular irrep is expanded in the specific active space of that irrep. The active spaces for all four irreps comprise 13 orbitals to be populated by 10 electrons, and can therefore be abbreviated as (10i13).

An improved correspondence between calculation and experiment, especially for the tungsten complex, can be reached by taking into account spin−orbit coupling. Due to the technical implementation of spin−orbital coupling in the MOLCAS program all states that are involved in such a calculation must be described at the CASSCF level with the same active space.[49] For this reason we recalculated all relevant ligand-field states with a smaller active space, which includes the five different d orbitals only. For the complexes at hand this results in distributing the two d electrons among five orbitals: (2i5) active space. The transition energies obtained in this way will be compared with the peak positions of the experimental spectra.

Results

The dodecahedral or square antiprismatic crystal field lifts the degeneracy of the d shell of the metal cations. The resulting pattern depends not only on the geometrical shape of the ligand cluster but also on the specific interaction between the ligand and metal cation. In semiempirical

(47) Hendrickx, M. F. A.; Mironov, V. S.; Chibotaru, L. F.; Ceulemans, A. *J. Am. Chem. Soc.* **2003**, *125*, 3694.
(48) Barandiaran, Z.; Seijo, L.; Huzinaga, S. *J. Chem. Phys.* **1990**, *93*, 5843.
(49) Malmqvist, P. A.; Roos, B. O.; Schimmelpfennig, B. *Chem. Phys. Lett.* **2002**, *357*, 230.

Table 2. CASPT2 (10i13) Results for the Dodecahedral and Square Antiprismatic isomers of $[Mo(CN)_8]^{4-}$ [a]

dodecahedron			square antiprism		
excited state	nature of transition	excitation energy	excited state	nature of transition	excitation energy
^1A	LF: $(x^2-y^2)\rightarrow(z^2)$	22015	^1A	LF: $z^2\rightarrow x^2-y^2$	26106
	MLCT: $(x^2-y^2)\rightarrow\pi^*$	32562		MLCT: $z^2\rightarrow\pi^*$	35879
	MLCT: $(x^2-y^2)\rightarrow\pi^*$	41329		MLCT: $z^2\rightarrow\pi^*$	44619
$^1B_1$	LF: $(x^2-y^2)\rightarrow(xy)$	38070	$^1B_1$	LF: $z^2\rightarrow xy$	25833
	MLCT: $(x^2-y^2)\rightarrow\pi^*$	42599		MLCT: $z^2\rightarrow\pi^*$	44154
	MLCT: $(x^2-y^2)\rightarrow\pi^*$	40335		MLCT: $z^2\rightarrow\pi^*$	40989
	MLCT: $(x^2-y^2)\rightarrow\pi^*$	40360		MLCT: $z^2\rightarrow\pi^*$	44736
$^1B_{2,3}$	LF: $(x^2-y^2)\rightarrow(xz,yz)$	33093	$^1B_{2,3}$	LF: $z^2\rightarrow xz,yz$	36291
	MLCT: $(x^2-y^2)\rightarrow\pi^*$	43753		MLCT: $z^2\rightarrow\pi^*$	42567
	MLCT: $(x^2-y^2)\rightarrow\pi^*$	39932		MLCT: $z^2\rightarrow\pi^*$	40548
	MLCT: $(x^2-y^2)\rightarrow\pi^*$	44146		MLCT: $z^2\rightarrow\pi^*$	40626
^3A	LF: $(x^2-y^2)\rightarrow(z^2)$	19413	^3A	LF: $z^2\rightarrow x^2-y^2$	23136
	MLCT: $(x^2-y^2)\rightarrow\pi^*$	32016		MLCT: $z^2\rightarrow\pi^*$	35347
	MLCT: $(x^2-y^2)\rightarrow\pi^*$	38760		MLCT: $z^2\rightarrow\pi^*$	42231
$^3B_1$	LF: $(x^2-y^2)\rightarrow(xy)$	35126	$^3B_1$	LF: $z^2\rightarrow xy$	23232
	MLCT: $(x^2-y^2)\rightarrow\pi^*$	42307		MLCT: $z^2\rightarrow\pi^*$	38342
	MLCT: $(x^2-y^2)\rightarrow\pi^*$	39638		MLCT: $z^2\rightarrow\pi^*$	43288
	MLCT: $(x^2-y^2)\rightarrow\pi^*$	39716		MLCT: $z^2\rightarrow\pi^*$	43119
$^3B_{2,3}$	LF: $(x^2-y^2)\rightarrow(xz,yz)$	30009	$^3B_{2,3}$	LF: $z^2\rightarrow xz,yz$	33126
	MLCT: $(x^2-y^2)\rightarrow\pi^*$	43056		MLCT: $z^2\rightarrow\pi^*$	42189
	MLCT: $(x^2-y^2)\rightarrow\pi^*$	38346		MLCT: $z^2\rightarrow\pi^*$	39502
	MLCT: $(x^2-y^2)\rightarrow\pi^*$	42663		MLCT: $z^2\rightarrow\pi^*$	39765

[a] All ligand-field (LF) transitions are calculated as individual CASSCF roots, whereas state averaged CASSCF wave functions were used for the MLCT transitions. States are classified according to the D_2 point group, all transition energies in wavenumbers.

methods, as applied in the original paper[22] to the title complexes, this pattern and the extent of splitting were acquired from a fitting procedure of a set of parameters (ligand-field parameters σ, π, and to some degree the Racah repulsion parameters B and C) to transition energies of the experimental spectra, with no assurance that the supposed natures of the various excited states were correct. This ligand-field parametrization, although 40 years old, is still the major source of information about the electronic structure of these complexes and related mononuclear fragments of magnetic clusters and networks. In the present study, we extract new parameters but now from calculated total energies. The advantage of our approach is that the expected accuracy of a few thousand wavenumbers for the excitation energies will allow us to assign with great certainty the true nature of the various experimental bands. In comparison with previous studies,[22,41] it will become clear that our theoretical analysis leads to a completely different interpretation of the spectra and a more reliable description of the electronic structure of these d^2 complexes.

Applying the (10i13) active spaces in CASPT2 calculations on $[Mo(CN)_8]^{4-}$ and $[W(CN)_8]^{4-}$ results in transition energies that are collected in Tables 2 and 3, respectively. Both complexes in both isomeric forms exhibit a low-spin singlet ground state. This is consistent with the fact that in a strong ligand-field created by cyanide ligands two electrons tend to pair in the lowest well-isolated nondegenerate d orbital. In the case of the dodecahedral structure, the two d electrons occupy the x^2-y^2 orbital, whereas in the square antiprismatic isomer the ground state is obtained by placing the two metal electrons in the z^2 orbital. The excitation energies in Tables 2 and 3 for the various excited states of a particular symmetry are obtained by calculating the ground states with the active space of that symmetry. It has been shown that such an approach has been successfully applied to the electronic spectra of a wide range of transition metal complexes[43−46] and molybdenum complexes in particular.[23,47] As can be deduced from these tables, the two isomers of both complexes have in common that the lowest states are calculated to be ligand-field states. The excitation from the ground state to these states involves the promotion of an electron from the lowest d orbital, i.e., x^2-y^2 for the dodecahedral complexes and z^2 in the case of the square antiprismatic shaped anions, to a higher positioned d orbital. Without any exception, all these ligand-field or d−d transitions are situated at energies lower than 40000 cm^{-1}.

Around 40000 cm^{-1} we encounter typical charge transfer transitions. In particular the spectroscopic important singlet charge transfer states $^1B_{2,3}$, which give rise to symmetry allowed intense absorption bands, can be found in an energy range 40000−50000 cm^{-1}. Not a single CT is found below 32000 cm^{-1} above the ground states. Analyses of the wave functions revealed that all CT states result from a promotion of an electron from the lowest lying metal d orbital to the $2\pi^*$ ligand orbital and therefore can be described as metal to ligand charge transfer transitions (MLCTs). This finding is just the opposite of the result obtained for $[Mo(CN)_8]^{3-}$ where the lowest transitions in the spectrum are characterized as a charge transfer transition of the type LMCT.[23] For the latter complex, ligand-field transitions fall in the same energy region as the CT transitions and, because of their low intensity, are masked in the experimental spectrum. The completely different assignment for the d^2 complexes is due to two reasons. First, the lowest d orbital for the M(IV) complexes is doubly occupied so that the electron in an LMCT excitation must be promoted to the next-lowest d level, which raises the excitation energy by more 20000 cm^{-1}. Second, the formal oxidation state of +4 of the metal

Table 3. CASPT2 (10i13) Results for the Dodecahedral and Square Antiprismatic Isomers of $[W(CN)_8]^{4-}$ [a]

dodecahedron			square antiprism		
excited state	nature of transition	excitation energy	excited state	nature of transition	excitation energy
^1A	LF: $(x^2-y^2)\rightarrow(z^2)$	19967	^1A	LF: $z^2\rightarrow x^2-y^2$	24715
	MLCT: $(x^2-y^2)\rightarrow\pi^*$	32990		MLCT: $z^2\rightarrow\pi^*$	33983
	MLCT: $(x^2-y^2)\rightarrow\pi^*$	45228		MLCT: $z^2\rightarrow\pi^*$	47258
$^1B_1$	LF: $(x^2-y^2)\rightarrow(xy)$	38632	$^1B_1$	LF: $z^2\rightarrow xy$	24152
	MLCT: $(x^2-y^2)\rightarrow\pi^*$	45566		MLCT: $z^2\rightarrow\pi^*$	42877
	MLCT: $(x^2-y^2)\rightarrow\pi^*$	42936		MLCT: $z^2\rightarrow\pi^*$	44744
	MLCT: $(x^2-y^2)\rightarrow\pi^*$	49788			
$^1B_{2,3}$	LF: $(x^2-y^2)\rightarrow(xz, yz)$	30627	$^1B_{2,3}$	LF: $z^2\rightarrow xz, yz$	36528
	MLCT: $(x^2-y^2)\rightarrow\pi^*$	42093		MLCT: $z^2\rightarrow\pi^*$	43098
	MLCT: $(x^2-y^2)\rightarrow\pi^*$	42766		MLCT: $z^2\rightarrow\pi^*$	42767
	MLCT: $(x^2-y^2)\rightarrow\pi^*$	49896		MLCT: $z^2\rightarrow\pi^*$	42178
^3A	LF: $(x^2-y^2)\rightarrow(z^2)$	18006	^3A	LF: $z^2\rightarrow x^2-y^2$	22969
	MLCT: $(x^2-y^2)\rightarrow\pi^*$	32556		MLCT: $z^2\rightarrow\pi^*$	32827
	MLCT: $(x^2-y^2)\rightarrow\pi^*$	40088		MLCT: $z^2\rightarrow\pi^*$	46028
	MLCT: $(x^2-y^2)\rightarrow\pi^*$	42660		MLCT: $z^2\rightarrow\pi^*$	43678
$^3B_1$	LF: $(x^2-y^2)\rightarrow(xy)$	37301	$^3B_1$	LF: $z^2\rightarrow xy$	22427
	MLCT: $(x^2-y^2)\rightarrow\pi^*$	42610		MLCT: $z^2\rightarrow\pi^*$	43627
	MLCT: $(x^2-y^2)\rightarrow\pi^*$	42088		MLCT: $z^2\rightarrow\pi^*$	41519
	MLCT: $(x^2-y^2)\rightarrow\pi^*$	44257		MLCT: $z^2\rightarrow\pi^*$	43749
$^3B_{2,3}$	LF: $(x^2-y^2)\rightarrow(xz, yz)$	29111	$^3B_{2,3}$	LF: $z^2\rightarrow xz, yz$	35031
	MLCT: $(x^2-y^2)\rightarrow\pi^*$	41912		MLCT: $z^2\rightarrow\pi^*$	43010
	MLCT: $(x^2-y^2)\rightarrow\pi^*$	40654		MLCT: $z^2\rightarrow\pi^*$	40825
	MLCT: $(x^2-y^2)\rightarrow\pi^*$	43734		MLCT: $z^2\rightarrow\pi^*$	42015

[a] All ligand-field (LF) transitions are calculated as individual CASSCF roots, whereas state averaged CASSCF wave functions were used for the MLCT transitions. States are classified according to the D_2 point group, all transition energies in wavenumbers.

cations in the d^2 complexes shifts the d orbitals upward with respect to the d orbitals of the M(V) complexes. The combination of these two factors gives rise to higher LMCT (above 40000 cm^{-1}) in the M(IV) octacyanocomplexes. These observations agree with the well-known fact that in the series of isostructural heterovalent complexes of the same element (such as MnO_4^-, MnO_4^{2-}, MnO_4^{3-}, or CrO_4^{2-}, CrO_4^{3-}) LMCT energies decrease with the increasing oxidation state.[50]

In order to get an idea about the absorption intensities of the various transitions, oscillator strengths were determined by calculating the transition dipole moment integrals at the CASSCF level. As can be expected, certain charge transfer transitions are found to possess oscillator strengths that are much larger than any ligand-field transitions. The most intense charge transfer absorption is at least 2 orders of magnitude stronger than the most intense d−d excitation. In the region between 40000 and 45000 cm^{-1}, our calculations even predict several strong CT absorptions for the dodecahedral as well as for the square antiprismatic isomers of both complexes. In this energy interval, both isomers of $[Mo(CN)_8]^{4-}$ exhibit CT transitions with oscillator strengths of about 0.30, whereas in the same interval somewhat larger oscillator strengths of about 0.40 are obtained for the two tungsten isomers. This reflects the experimentally observed trend of the extinction coefficients for the two complexes in aqueous solution.[22] Indeed, an extinction coefficient of 15540 is reported for the transition at 41670 cm^{-1} in the molybdenum complex, and a much larger value of 25060 at 40160 cm^{-1} is reported for $[W(CN)_8]^{4-}$. These experimental transition energies are satisfactorily reproduced by our CASPT2 results, as is testified by Tables 2 and 3. The average oscillator strength of 0.3 for $[Mo(CN)_8]^{4-}$ is much larger than the values (between 0.02 and 0.064) calculated by us recently[23] for $[Mo(CN)_8]^{3-}$ and matches the observation that the extinction coefficients for the latter complex are considerably smaller (ϵ values between 1350 and 2000).

The CASPT2 results obtained for ligand-field states by utilizing the smaller (2i5) active space are collected in Tables 4 and 5 for $[Mo(CN)_8]^{4-}$ and $[W(CN)_8]^{4-}$, respectively. When comparing these results with those for the larger active space, as depicted in Figures 2 and 3, we must conclude that the differences are rather small. For all ligand-field states, they are less than 1000 cm^{-1}. Therefore, the smaller active space can equally well be used for the description of the electronic structure of the four structures. A possible reason for this finding is that the energetic position of the d orbitals is almost exactly in the middle of the 1π and $2\pi^*$ orbitals of the cyanide ligand. Indeed, the large energy gap between these orbitals as a consequence of the strong triple bond of the free cyanide results in small contributions in the CASSCF wave functions. The CASPT2 energies of the (2i5) active space were subsequently used as diagonal elements in the spin−orbital coupling calculations. The off-diagonal interaction elements between the various terms were evaluated by using the CASSCF wave functions of the same active space. This procedure has recently been applied successfully.[49] The results of this computational approach for the present d^2 octacyanocomplexes are also shown in Tables 4 and 5. As could be expected, the difference induced by taking into account spin−orbital coupling effects is indeed small for the $[Mo(CN)_8]^{4-}$ complex. For the dodecahedral isomer as well as for the square antiprismatic isomer, the general features of the CASPT2 ligand-field spectrum are nearly completely retained. A graphical representation of the results depicting this finding is shown in Figure 2. The splitting of the various

(50) Lever, A. B. P. *Inorganic Electronic Spectroscopy*, 2nd ed.; Elsevier: Amsterdam, 1984.

Table 4. CASPT2 (2i5) and Spin−Orbital Coupling (SOC) Results for $[Mo(CN)_8]^{4-}$ [a]

dodecahedron						square antiprism					
			SOC			SOC					
state		CASPT2 (2i5)		singlet	triplet	singlet	triplet		CASPT2 (2i5)	state	
D_{2d}	D_2	ΔE	ΔE	contribution	contribution	contribution	contribution	ΔE	ΔE	D_2	D_{4d}
$^1A_1$	^1A	0	0	100	0	100	0	0	0	^1A	$^1A_1$
$^3B_1$	^3A	19673	19621	0	100	0	100	22977	23570	^3A	$^3E_2$
			19640	0	100	0	100	22978	24185	$^3B_1$	
			19640	0	100	7	93	23353			
						14	86	23852			
$^1B_1$	^1A	22075	22011	98	2	0	100	24831			
						0	100	24831			
^3E	$^3B_{2,3}$	30051	29722	0	100						
			29734	2	98	85	15	26277	25902	^1A	$^1E_2$
			30086	1	99	92	8	26550	26287	$^1B_1$	
			30086	1	99						
			30551	0	100	0	100	32723	33177	$^3B_{2,3}$	$^3E_3$
			30566	0	100	0	100	32788			
						2	98	33146			
^1E	$^1B_{2,3}$	33264	33301	94	6	2	98	33218			
			33301	94	6	0	100	33767			
						0	100	33772			
$^3A_2$	$^3B_1$	35252	35452	0	100						
			35469	5	95	98	2	36915	36754	$^1B_{2,3}$	$^1E_3$
			35469	5	95	98	2	36918			
$^1A_2$	$^1B_1$	38568	38688	99	1						

[a] All transition energies (ΔE) in wavenumbes, singlet and triplet contributions to the SOC wave functions in percentage.

Table 5. CASPT2 (2i5) and Spin−Orbital Coupling (SOC) Results for $[W(CN)_8]^{4-}$ [a]

dodecahedron						square antiprim					
			SOC			SOC					
state		CASPT2 (2i5)		singlet	triplet	singlet	triplet		CASPT2 (2i5)	state	
D_{2d}	D_2	ΔE	ΔE	contribution	contribution	contribution	contribution	ΔE	ΔE	D_2	D_{4d}
$^1A_1$	^1A		0	98	2	98	2	0		^1A	$^1A_1$
$^3B_1$	^3A	18123	17900	0	100	1	99	20499	22577	^3A	$^3E_2$
			18001	2	98	1	99	20499	22672	$^3B_1$	
			18001	2	98	35	65	21173			
						34	66	21352			
$^1B_1$	^1A	20094	19942	93	7	0	100	25468			
						0	100	25468			
^3E	$^3B_{2,3}$	30055	30041	7	93						
			30112	0	100	64	36	25977	23884	$^1B_1$	$^1E_2$
			30504	12	88	65	35	26107	24028	^1A	
			30504	12	88						
			31423	6	94	0	100	34420	35287	$^3B_{2,3}$	$^3E_3$
			31667	1	99	2	98	34970			
						27	73	35101			
^1E	$^1B_{2,3}$	31471	32231	81	19	27	73	35101			
			32231	81	19	1	99	37596			
						1	99	37666			
$^3A_2$	$^3B_1$	37437	38582	5	95						
			38582	5	95	72	28	38631	36963	$^1B_{2,3}$	$^1E_3$
			38781	1	99	72	28	38631			
$^1A_2$	$^1B_1$	38492	39521	94	6						

[a] All transition energies (ΔE) in wavenumbes, singlet and triplet contributions to the SOC wave functions in percentage.

singlet and triplet terms is the largest for the triplet states of the square antiprism and amounts to about 2000 cm^{-1}. Nevertheless, Table 4 clearly demonstrates that the spin quantum number is conserved to a fairly large extent. The triplet−singlet mixing remains limited to 6% and 15% in the case of the electronic states of the dodecahedron and the square antiprism, respectively. For the two isomeric forms of the $[W(CN)_8]^{4-}$ complex, the effects of the spin−orbit coupling are definitely more pronounced. This is witnessed by the larger splitting of the triplet CASPT2 terms, which now also notably affects the dodecahedron, although still to a lesser extent than the square antiprism. In the latter isomer, the lowest excited singlet and triplet terms $^{1,3}A$ and $^{1,3}B_1$, both components of the $^{1,3}E_2$ (D_{4d}), are strongly mixed. The energy difference between the $^1E_2$ and $^3E_2$ terms of about 1300 cm^{-1} at the CASPT2 level is more than quadrupled to about 5500 cm^{-1} by incorporating spin−orbit coupling. Table 5 shows that the singlet−triplet mixing in these states is as high as 35%, which is more than twice the mixing obtained for the same states of the same isomer of the molybdenum complex. These observations are consistent with the fact that the spin−orbit coupling for 5d electrons is generally much stronger than for 4d electrons. Larger spin−orbit splitting of the energy levels in the square antiprismatic complexes

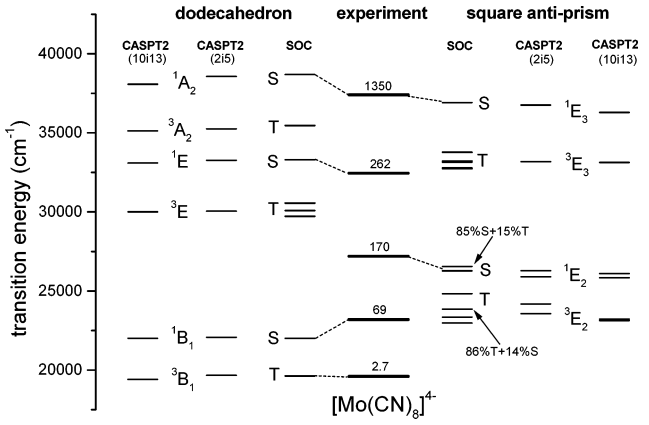

Figure 2. Comparison of ab initio (CASPT2 and spin−orbital coupling transition energies) results for $[Mo(CN)_8]^{4-}$ with experimental data.[22] Numbers at experimental transition energies are the extinction coefficients at peak position of the corresponding absorption bands.

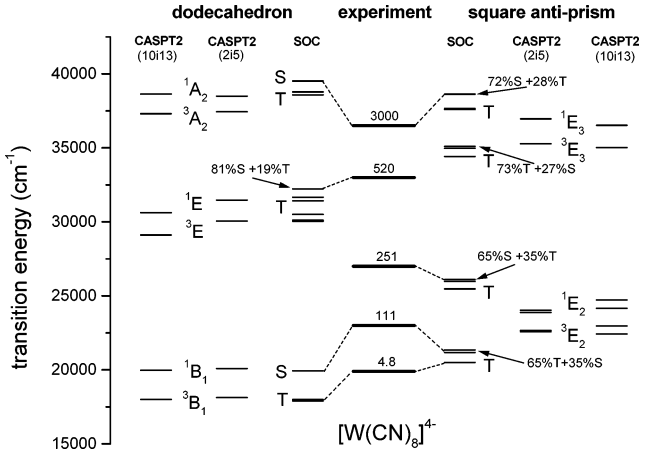

Figure 3. Comparison of ab initio (CASPT2 and spin−orbital coupling transition energies) results for $[W(CN)_8]^{4-}$ with experimental data.[22] Numbers at experimental transition energies are the extinction coefficients at peak position of the corresponding absorption bands.

is related to the unquenched orbital momentum in the upper ($x^2 - y^2$, xy) and (xz, yz) doubly degenerate orbital levels (Figure 4). As a result, the first-order spin−orbit splitting of triplet states takes place in the antiprismatic complexes while in the dodecahedral complexes they split in the second-order.

Discussion

The data as presented in Tables 4 and 5 allow us to propose an assignment of the low-energy bands in the experimental spectrum. An overview of our proposed assignment of the ligand-field spectra for the molybdenum and tungsten complexes is given in Table 6. In this table the transitions are not only classified according to the D_2 point group that is used in our CASPT2 calculations, but also according to the actual symmetry of the dodecahedral (D_{2d}) and the square antiprism isomers (D_{4d}). The assignments are also depicted in Figures 2 and 3 as dashed lines that connect the theoretical (CASPT2 energies corrected for spin−orbit interaction) energetic positions of the various excited states and the experimental transition energies, which are in the middle of Figures 2 and 3. The lowest transition occurs in both

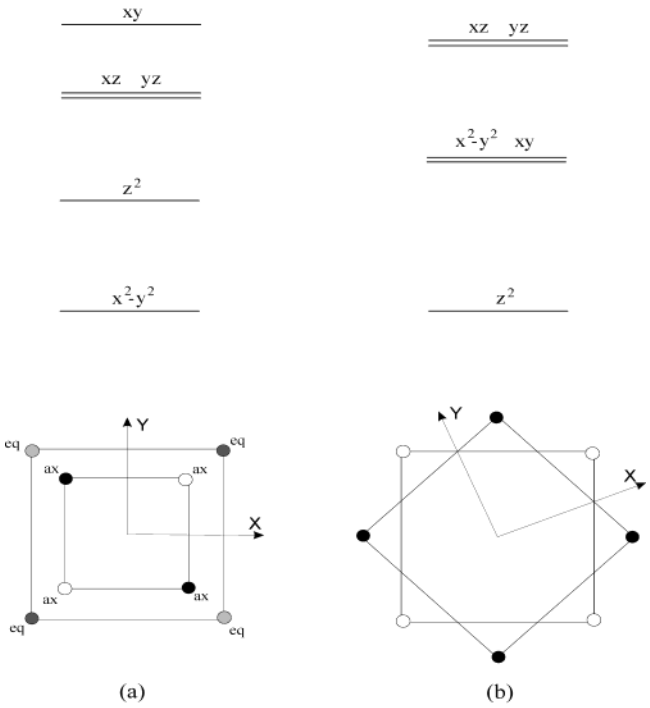

Figure 4. Qualitative orbital pattern for the d orbitals of the dodecahedral (a) and square antiprismatic isomers (b). Black and white circles indicate ligands at positions at a larger distance above or beneath the *xy* plane, respectively. Dark or light gray circles symbolize ligands at a shorter distance above or beneath the *xy* plane, respectively.

complexes at energies slightly lower than 20000 cm^{-1}. The very low extinction coefficients for these transitions in comparison with the other ligand-field transitions suggest spin-forbidden transitions from the singlet ground states to triplet excited states. For the molybdenum complex, the most likely assignment is a transition to the lowest triplet ligand-field state of the dodecahedral isomer, which involves an excitation of an electron from the $x^2 - y^2$ orbital to z^2. For this complex, the lowest triplet states (^3A and $^3B_1$) of the square antiprism isomer are situated at about 23000 cm^{-1} and, given the accuracy of a few thousand wavenumbers, should be ruled out to contribute to the experimental band that is situated at 19600 cm^{-1}. In the tungsten complex, this weak transition is located slightly higher at 19900 cm^{-1}. Figure 3 shows that the best match here is the lowest triplet state (^3A and $^3B_1$ as components of $^3E_2$ (D_{4d})) of the square antiprism. Quite interesting is the fact that the spin−orbit interaction shifts this term downward for about 2000 cm^{-1}, placing it almost exactly at the experimental band position. However, the lowest triplet state of the dodecahedron isomers is calculated at 18000 cm^{-1} and could, given an error margin of a few thousand wavenumbers for our calculations, also contribute to the experimental low-intensity band at 19900 cm^{-1}. The second lowest transition in the experimental spectra of the complexes is located at about 23000 cm^{-1} or slightly above. Its intensity is higher than the lowest transition, which suggests a spin-allowed ligand-field transition. For the molybdenum complex, the most likely candidate is the $x^2 - y^2 \rightarrow z^2$ transition of the dodecahedron that is calculated in the vicinity of 22000 cm^{-1}. For the tungsten complex, the same transition is probably accountable for this

Table 6. Assignment of the Experimental Band Positions[22] for $[Mo(CN)_8]^{4-}$ and $[W(CN)_8]^{4-}$ [a]

$[Mo(CN)_8]^{4-}$						
dodecahedron				square antiprism		
D_{2d}	D_2		experiment		D_2	D_{4d}
$^1A_1 \rightarrow {}^3B_1$	$^1A \rightarrow {}^3A$	$x^2-y^2 \rightarrow z^2$	19600 (2.7)			
$^1A_1 \rightarrow {}^1B_1$	$^1A \rightarrow {}^1A$	$x^2-y^2 \rightarrow z^2$	23200 (69)			
			27200 (170)	$z^2 \rightarrow (x^2-y^2, xy)$	$^1A \rightarrow {}^1A, {}^1B_1$	$^1A_1 \rightarrow {}^1E_2$
$^1A_1 \rightarrow {}^1E$	$^1A \rightarrow {}^1B_2, {}^1B_3$	$x^2-y^2 \rightarrow (xz, yz)$	32450 (262)			
$^1A_1 \rightarrow {}^1A_2$	$^1A \rightarrow {}^1B_1$	$x^2-y^2 \rightarrow xy$	37400 (1350)	$z^2 \rightarrow (xz, yz)$	$^1A \rightarrow {}^1B_2, {}^1B_3$	$^1A_1 \rightarrow {}^1E_3$
		MLCT	41670 (15540)	MLCT		
$[W(CN)_8]^{4-}$						
dodecahedron				square antiprism		
D_{2d}	D_2		experiment		D_2	D_{4d}
$^1A_1 \rightarrow {}^3B_1$	$^1A \rightarrow {}^3A$	$x^2-y^2 \rightarrow z^2$	19900 (4.8)	$z^2 \rightarrow (x^2-y^2, xy)$	$^1A \rightarrow {}^3A, {}^3B_1$	$^1A_1 \rightarrow {}^3E_2$
$^1A_1 \rightarrow {}^1B_1$	$^1A \rightarrow {}^1A$	$x^2-y^2 \rightarrow z^2$	23000 (111)	$z^2 \rightarrow (x^2-y^2, xy)$	$^1A \rightarrow {}^1A, {}^1B_1$	$^1A_1 \rightarrow {}^1E_2$
			27000 (251)	$z^2 \rightarrow (x^2-y^2, xy)$	$^1A \rightarrow {}^1A, {}^1B_1$	$^1A_1 \rightarrow {}^1E_2$
$^1A_1 \rightarrow {}^1E$	$^1A \rightarrow {}^1B_2, {}^1B_3$	$x^2-y^2 \rightarrow (xz, yz)$	33000 (520)			
$^1A_1 \rightarrow {}^1A_2$	$^1A \rightarrow {}^1B_1$	$x^2-y^2 \rightarrow xy$	36500 (3000)	$z^2 \rightarrow (xz, yz)$	$^1A \rightarrow {}^1B_2, {}^1B_3$	$^1A_1 \rightarrow {}^1E_3$
		MLCT	40160 (25060)	MLCT		

[a] Peak positions in wavenumbers, numbers in parentheses are the corresponding extinction coefficients.

band, although the correspondence between theoretical and experimental excitation energies is not as good. Also, a contribution from the spin−orbit states at 21173 and 21352 cm^{-1} (Table 5) is possible. These states have indeed a large singlet contribution which matches the larger experimental extinction coefficient ($\epsilon = 111$). The bands at about 27000 cm^{-1} in both complexes are beyond any doubt to be attributed to the square antiprism isomers. Again, their relatively high intensities suggest spin-allowed ligand-field transitions. After taking into account spin−orbit coupling effects, the $z^2 \rightarrow (x^2 - y^2, xy)$ ($^1A_1 \rightarrow {}^1E_2$ (D_{4d})) transitions are in both complexes calculated between 26000 and 26500 cm^{-1} (Tables 4 and 5). The nearest singlet states of the dodecahedral isomers of both complexes are $^1B_{2,3}$, both components of the ^1E (D_{2d}) states. They are positioned well above 30000 cm^{-1}, namely at 33300 and 32200 cm^{-1} for the molybdenum and tungsten complexes, respectively, and are therefore not engaged in the absorption at 27000 cm^{-1}. Furthermore, from Figures 2 and 3 it follows that these states are solely to be held responsible for the experimental bands at 32450 cm^{-1} of $[Mo(CN)_8]^{4-}$ and 33000 cm^{-1} of $[W(CN)_8]$.$^{4-}$ These bands therefore correspond to $x^2 - y^2 \rightarrow (xz, yz)$ transitions in the dodecahedron isomers. The highest energy bands at 37400 cm^{-1} for the molybdenum complex and at 36500 cm^{-1} for the tungsten complex contain in both cases contributions from the dodecahedral and square antiprismatic isomers. For the latter isomer, the transition $z^2 \rightarrow (xz, yz)$ is responsible for this band, and therefore, the excited state involved is orbitally degenerate ($^1E_3$). For the dodecahedron, the relevant excited state for this band is nondegenerate since the electron is promoted to the *xy* orbital of the metal. The high extinction coefficient of this band ($\epsilon = 1350$ (Mo) and $\epsilon = 3000$(W)) is probably due to interactions (intensity stealing) with close by charge transfer transitions. This may also be the case for the bands at 32450 ($\epsilon = 262$) and 33000 ($\epsilon = 520$) cm^{-1} of the molybdenum and tungsten complexes, respectively. Indeed, in this region there are some MLCT transitions, which are either spin or Laporte forbidden (Tables 2 and 3).

On the basis of the complete résumé of our assignment of the experimental spectra of the two title complexes as given in Table 6, we can draw a very important conclusion. According to our theoretical results, the presence of an absorption band at 27200 cm^{-1} (Mo) and 27000 cm^{-1} (W) unambiguously proves the presence of the square antiprismatic isomer in solutions, whereas the absorption bands at 32450 cm^{-1} (Mo) and 33000 cm^{-1} (W) are due to the dodecahedral structures of both complexes. Therefore, we must assume that the experimental spectra are the superposition of the individual spectra of the two isomers. This means that in aqueous solutions the two isomeric forms of the tetravalent octacyanocomplexes of molybdenum and tungsten are in dynamic equilibrium:

$$\text{dodecahedron} \rightleftharpoons \text{square antiprism}$$

As mentioned in the Introduction, these two structures are frequently encountered in X-ray analysis of crystal structures of these complexes. Apparently, the two isomers of the complex anions are almost equally stable so that the actual structure in a crystal is determined by the nature of the counterions. This is further corroborated by the total energies that we have calculated for the ground states of the various structures. For $[Mo(CN)_8]^{4-}$ and $[W(CN)_8]^{4-}$, the difference between the ground states of the two isomers is about 4 kcal/mol (D_{4d} isomer lower than D_{2d} isomer), which points to an equilibrium between them.

The fact that the experimental absorption spectrum is the result of electronic excitations taking place in the two isomers does not prevent us from summarizing the electronic structure of them in terms of common sets of the ligand-field, spin−orbit coupling, and Racah parameters. This is in line with the transferability postulate of the angular overlap model. For the molybdenum complexes, the following set of parameters was obtained: $e_\sigma = 25857\ cm^{-1}$, $e_\pi = 8754\ cm^{-1}$,

$\zeta = 600\ cm^{-1}$, $B = 180\ cm^{-1}$, and $C = 1000\ cm^{-1}$. The values $e_\sigma = 19833\ cm^{-1}$, $e_\pi = 3685\ cm^{-1}$, $\zeta = 2000\ cm^{-1}$, $B = 100\ cm^{-1}$, and $C = 400\ cm^{-1}$ gave the best fit for the tungsten isomers. The qualitative orbital pattern for the ligand-field splitting of the d orbitals as it emerges from our CASPT2 transition energies is depicted in Figure 4. In contradiction with the semiempirical treatment of reference 22, the *xy* orbital of the dodecahedral isomer is found by our calculations as the highest energy d orbital. The antibonding interaction of this orbital with the equatorial ligands that are placed either slightly above (dark gray colored in Figure 4a) or slightly underneath (light gray colored) the *xy* plane is responsible for its highest position among the d orbitals. In the square antiprismatic isomer, all ligands are positioned at higher locations with respect to the *xy* plane and are simultaneously rotated in the direction of the *x* and *y* axes, so that the *xy* orbital is becoming less antibonding and therefore shifted to lower energies. For the *xz* and *yz* orbitals, the opposite situation occurs (increase of antibonding character), and these orbitals are more destabilized in the square antiprism; in fact, they have become the highest in energy.

The smaller Racah parameters *B* and *C* for the tungsten complexes are illustrated in Figures 2 and 3 by the fact that the triplet−singlet splitting of the d^2 configurations are much smaller in the tungsten isomers (Figure 3) than in the analogue molybdenum structures (Figure 2). This has some bearing on the explanation of the magnetic effects of compounds possessing octacyanocomplexes as building blocks. In particular, this can account for the difference in the magnetic behavior of isostructural and isoelectronic $M_6Mn_9(CN)_x$ cyano-bridged clusters based on the $[M(CN)_8]^{3-}$ d^1 complexes (M = Mo or W). The molybdenum cluster is ferromagnetic while the tungsten counterpart is antiferromagnetic.[51,52] The ferromagnetic contribution to the exchange interaction in $M^V-CN-Mn^{II}$ fragments was shown to be crucially dependent on the I/U ratio,[20] where *U* is the metal-to-metal electron promotion energy and *I* is the intraionic Hund's rule coupling parameter on *M*; the latter can be estimated via the Racah parameters as $I \approx 2C + 6B$.[53] Therefore, much smaller *B* and *C* parameters found for the tungsten octacyanometalate seem to be responsible for the origin of antiferromagnetism in $W^V-CN-Mn^{II}$ exchange pairs.

Conclusion

Our CASPT2 calculations clearly assign the high-intensity absorption bands of $[Mo(CN)_8]^{4-}$ and $[W(CN)_8]^{4-}$ at energies above $40000\ cm^{-1}$ to charge transfer transitions of the type where an electron is promoted from the lowest lying metal d orbital to the unoccupied $2\pi^*$ orbitals of the cyanide ligand. This is just the opposite electron transfer of the active one in the lowest CTs of the related $[Mo(CN)_8]^{3-}$, which was recently demonstrated in our previous ab initio study on the latter complex. The calculated oscillator strengths are in agreement with the more intense CT absorption in $[Mo(CN)_8]^{4-}$ as compared to $[Mo(CN)_8]^{3-}$. An even more intense absorption band above $40000\ cm^{-1}$ for $[W(CN)_8]^{4-}$ as compared to the corresponding band of $[Mo(CN)_8]^{4-}$ is also predicted by our calculated oscillator strengths. All experimental bands below $40000\ cm^{-1}$ can be assigned to ligand-field transitions, although some MLCT contribution cannot be excluded. In order to account for all experimental transitions in the spectrum of the aqueous solutions of the complexes, an equilibrium between the dodecahedral and square antiprismatic isomers is proposed. The smaller singlet−triplet splitting of the ligand-field states for the tungsten complexes as reflected in the smaller Racah parameters *B* and *C* is related to the fact that the 5d orbitals of W(IV) are definitely more diffuse than the 4d orbitals of Mo(IV). This corroborates the proposed explanation[20] of the origin of ferromagnetic exchange interaction in heteronuclear cyanide-bridged clusters and networks containing d^1 octacyanometalates.

Acknowledgment. Financial support by the Belgian National Science foundation and Flemish Government under the Concerted Action Scheme, the Russian Foundation for Basic Research (Grant No. 01-02-32210), and the INTAS Grant 00-00565 is gratefully acknowledged.

IC035282T

(51) Larionova, J.; Gross, M.; Pilkington, M.; Anders, H.; Stoeckli-Evans, S.; Gudel, H. U. *Angew. Chem., Int. Ed.* **2000**, *39*, 1605.

(52) Zhong, Z. J.; Seino, H.; Mizobe, Y.; Hidai, M.; Fijishima, A.; Ohkoshi, S.-I.; Hashimoto, K. *J. Am. Chem. Soc.* **2000**, *122*, 2952.

(53) Griffith, J. S. *The Theory of Transition Metal Ions*; Cambridge University Press: Cambridge, 1971.